Available online at www.sciencedirect.com
ScienceDirect
Catalysis Today 123 (2007) 133–141
CATALYSIS TODAY
www.elsevier.com/locate/cattod

The activity and stability of Pd/C catalysts in benzene hydrogenation

Po-Hua Jen, Yin-Hou Hsu, Shawn D. Lin *

Department of Chemical Engineering and Material Science, Yuan Ze University, 135 Yuan-tung Road, Chung-Li 320, Taiwan, ROC

Available online 1 February 2007

Abstract

Carbon black supported Pd catalysts were prepared by an incipient wetness impregnation method and tested for benzene hydrogenation. The catalytic activity is subjected to serious deactivation. However, the deactivation is found to depend on the test procedure. When the reaction is performed under constant flow of benzene and hydrogen during a stepwise temperature-ascending-descending test sequence, no deactivation is observed. Deactivation occurs when the reaction gas is replaced by a He purge during temperature changes in the test sequence. The Pd/C catalysts prepared from different precursors show similar activation energy and similar TOF as oxide-supported Pd catalysts when deactivation is confined by applying suitable experimental procedures. EXAFS, TEM, and TGA results suggest that both Pd sintering and carbonaceous residue are responsible for the deactivation.

Keywords: Benzene; Hydrogenation; Pd/C; Deactivation; $PdCl_2$; $Pd(NO_3)_2$

1. Introduction

The hydrogenation of benzene and toluene have been studied extensively by Vannice and coworkers over supported Fe [1,2], Pd [3–10], and Pt [10–15] catalysts. Both reactions are structure-insensitive and all the metal catalysts show similar kinetic characteristics. The apparent activation energy usually falls within 10–12 kcal/mol. The reaction conversion as a function of reaction temperature shows a reversible volcano shape in vapor-phase reactions. This volcano-shape curve is not owing to catalyst deactivation or thermodynamic limitation. It can be successfully explained by a Langmuir–Hinshelwood mechanism, in which the benzene surface coverage is reduced with increase of temperature that eventually offsets the kinetic temperature effect [2,5].

The apparent reaction order on benzene (or toluene) on metal catalysts is usually zero order, though 0.5 order was also reported [4]. The apparent reaction order on hydrogen is found to increase with reaction temperature [1,4,10,12,13]. The reaction order on H_2 is found to 0.5 at lower reaction temperatures [12,13] while the order on H_2 as high as 4 [1,4] was observed at higher reaction temperatures. Vannice and coworkers have studied extensively the possible reaction mechanism of benzene and toluene hydrogenation by model fitting [2,5,8,10,14,15]. A Langmuir–Hinshelwood model involving H-deficient species from adsorbed benzene (or toluene) can fit reasonably with the measured kinetic data from both vapor-phase [14] and liquid-phase [15] reactions. This model suggests that the increase of apparent hydrogen reaction order with increase of reaction temperature is attributable to fewer H remained on the aromatic ring in the H-deficient surface species at higher temperature.

The reaction is structure insensitive and therefore the specific activity, in term of turnover frequency (TOF), and the activation energy is independent of metal particle size, precursor, or pretreatment [4]. However, acidic oxide supports resulted in metal catalysts with higher TOF than less acidic oxide supports [4,7,10–13], and it is attributed to the reaction occurring not only on the metal surface but also at the metal-support interfacial region [5]. On the other hand, carbon-supported Pd catalysts show somewhat different behavior from oxide-supported metal catalysts during benzene hydrogenation [4,9]. A volcano-shape conversion–temperature plot is still observed in the vapor-phase benzene hydrogenation over Pd/C, but experimental data show severe deactivation [16] and H_2 chemisorption is found to be suppressed [4,9,17,18]. In addition, the measured TOF and activation energy of the vapor-phase benzene hydrogenation over Pd/C catalysts are

* Corresponding author. Tel.: +886 3 4638800x2554; fax: +886 3 4559373.
E-mail address: sdlin@saturn.yzu.edu.tw (S.D. Lin).

0920-5861/$ – see front matter © 2007 Elsevier B.V. All rights reserved.
doi:10.1016/j.cattod.2007.01.033

lower than those of oxide-supported Pd catalysts [4]. The type of precursor was reported to affect the characteristics of Pd/C catalysts [18]. These results suggest that Pd/C catalysts may not be suitable for catalyzing benzene or toluene hydrogenation, and still Pd/C catalysts are widely used in the industry for various types of hydrogenation reactions including aromatic compounds. The present work examines the deactivation of Pd/C during vapor-phase benzene hydrogenation in order to determine when and how the deactivation of Pd/C occurs. It is found that the deactivation depends on the procedure of reaction test. Possible reasons for the deactivation are discussed in the present work.

2. Experimental

2.1. Catalyst preparation

The Pd/C catalysts were prepared by an incipient wetness impregnation method from aqueous solution of Pd precursor. Two Pd precursors ($PdCl_2$ (Aldrich, 99.999%) and $Pd(NO_3)_2{\cdot}2H_2O$ (Merck, 99.99%)) and two carbon black supports (Cabot, XC72 and XC72R, both after 1273 K N_2 passivation followed by activation with O_2 at 623 K) were used. The $PdCl_2$ precursor was dissolved in 0.1 M HCl to form H_2PdCl_4 solution for impregnation. The fresh catalyst was dried in an oven at 373 K for 4 h and then reduced either by on-line hydrogen treatment at 573 K or by an aqueous $NaBH_4$ (0.5%, diluted from Merck 99%) at 298 K. The latter reduction was performed by dropwise-addition of $NaBH_{4(aq)}$ to a catalyst suspension; the mixture was agitated for 24 h, then filtered, washed with deionized water, and dried at room temperature in a vacuum oven.

2.2. Catalyst characterization

The specific surface area and CO chemisorption measurements of the prepared catalysts were performed on ASAP 2000 (Micromeritics) instrument. The Pd dispersion is calculated based on the irreversible CO uptake from a dual-isotherm experiment and assuming a CO/Pd_s ratio of 1 [19]. Transmission electron microscopy was also used for catalyst characterization. Extended X-ray absorption fine structure (EXAFS) analysis was performed ex situ at room temperature, at the Pd K-edge using the BL01C beam line at National Synchrotron Radiation Research Center in Taiwan. The monochromator employed Si(1 1 1) crystals for energy selection. EXAFS experiments were conducted in transmission mode and the intensities of both incident and transmitted X-ray beams were measured by gas ionization chambers. The energy was scanned from 200 eV below the edge to 1000 eV above the edge. The raw absorption data, with pre-edge and post-edge backgrounds subtracted, were normalized to the edge jump to yield the EXAFS function. After being weighted by k^3 to compensate the damping of the EXAFS oscillations with increase of k (the photoelectron wave number), the EXAFS function was Fourier transformed to r-space in which a nonlinear least-squares fitting algorithm was applied. All the computer programs were implemented in the UWXAFS package [20]. The back-scattering amplitude and phase shift for specific atom pairs were theoretically calculated with FEFF7 code [21]. The amplitude factor was calibrated against measured data of reference samples such as Pd foil, $PdCl_2$ and $Pd(NO_3)_2$ and it was found to be within 7% error. Therefore, the fitting amplitude factors were used without further correction.

2.3. Activity tests

Vapor-phase benzene hydrogenation was carried out in a fixed-bed microreactor system, in which a 4-way valve was installed in front of the reactor for checking the gas composition before entering the reactor. Hydrogen (Sanfu, 99.995%) and helium (Sanfu, 99.995%) were further purified by passage through oxytraps and molecular sieve traps. Mass flow controllers were used to tune gas flow rates. Benzene (Merck, 99.8%) was fed into a heated line using a syringe pump, and was carried into the reactor by H_2/He flow. Typically 45 mg of catalyst was loaded in a Pyrex reactor and pretreated in line prior to reaction. The reaction conditions were 30 Torr (4 kPa) benzene, 500 Torr (66.6 kPa) H_2, balance He and at a space velocity of 66 μmol benzene/h/g catalyst. The reaction typically became steady-state after 5 min on stream and the average conversion from 25 to 40 min was recorded. A temperature-ascending-descending sequence was used in the test and a bracketing technique was applied in which the reaction gas was replaced by He purge during changes to the reaction temperature. This bracketing technique would cause partial restoration of active surface by reducing the concentration of adspeices. The reactor effluent was analyzed by gas chromatography (Shidmazu, GC-8A) with TCD detector and a Carbowax 20M packed column. Cyclohexane is the only product from the reactor. The TOF is calculated based on the Pd dispersion determined by CO chemisorption. The Weisz criterion [22] was checked and the catalysts were subjected to negligible mass transfer limitations.

3. Results

3.1. Benzene hydrogenation

The benzene conversion over a 10% Pd/C catalyst from two consecutive temperature-ascending-descending sequences is shown in Fig. 1. The activity versus temperature appears in volcano-shape with a peak activity occurring at around 460 K. Steady-state benzene conversion was observed at each test temperature, but the recorded conversion in the temperature-descending branch is lower than that in its preceding temperature-ascending branch. The Pd/C apparently suffers from deactivation. Such activity loss results in an irreversible volcano-shape in its activity–temperature plot, in contrast to a reversible volcano-shape often observed in oxide-supported metal catalysts [4,7,11,12,23]. The irreversible plot was shown in earlier reports of benzene hydrogenation over Pd/C catalysts [16] and is observed in all the Pd/C tested in this study when following the same bracketing technique. Such activity loss was

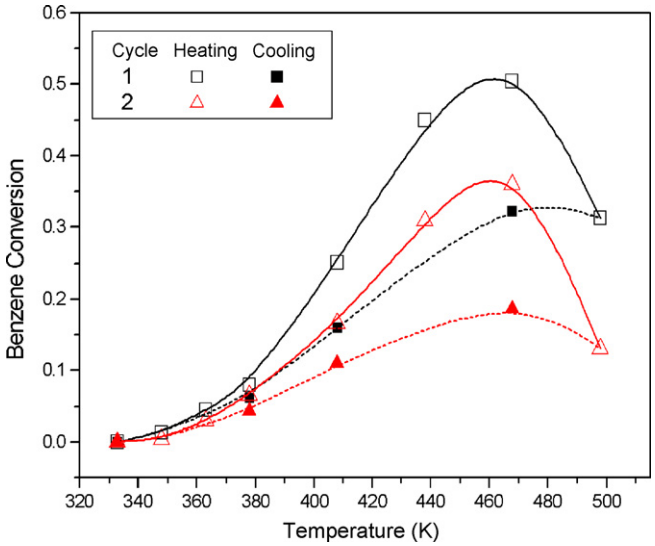

Fig. 1. Steady-state benzene conversion during a 2-cycle temperature-ascending-descending sequence of benzene hydrogenation over a 10% Pd/C catalyst. The Pd/C is prepared from $PdCl_2$ and XC72 support and is reduced by $NaBH_{4(aq)}$ followed by on-line H_2 reduction at 573 K. The catalyst was purged with He while changing the reaction temperature.

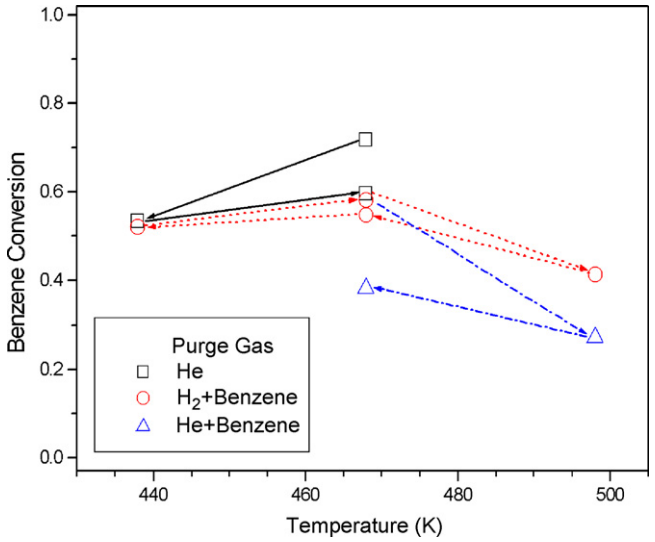

Fig. 3. Effect of purge gas composition during temperature variation on the steady-state benzene hydrogenation conversion over a 10% Pd/C catalyst. The Pd/C is prepared from $PdCl_2$ and XC72R carbon support, and has been subjected to a 20-h life test at 468 K reported in Fig. 2. Arrows indicate the sequence of measurement.

also observed in a shorter temperature-sequence up to only 453 K, and the activity loss was found more significant if the reaction temperature is higher [23]. Furthermore, deactivation was more severe, when more data points were recorded during a temperature-ascending sequence covering the same temperature range [24]. The activity and the stability of Pd/C during benzene hydrogenation appear to be dependent on test procedure. As a consequence, the activity reported later in this study is compared using identical test sequences.

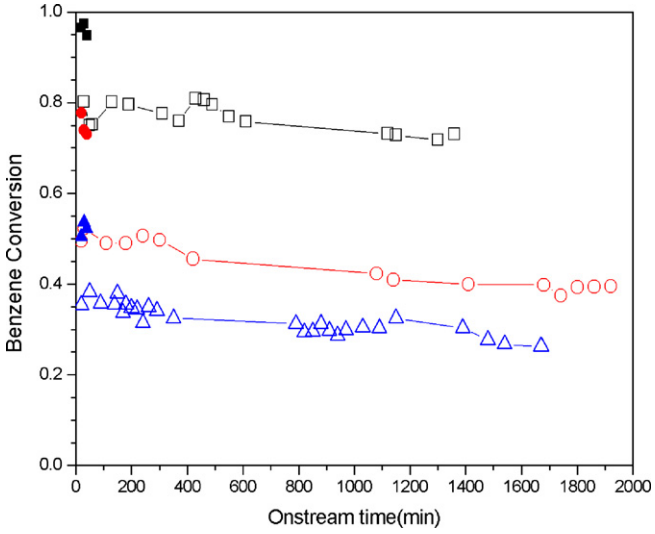

Fig. 2. The benzene conversion as a function of onstream time over 10% Pd/C catalysts at 468 K. The catalyst is prepared from $PdCl_2$ and XC72R (□, ■), $Pd(NO_3)_2$ and XC72R (○, ●), and $Pd(NO_3)_2$ and XC72 (△, ▲), respectively. All catalysts were reduced by $NaBH_{4(aq)}$ and then purged in line with He at 373 K before reaction test. Open symbols represent the data recorded directly at 468 K for the life test; the filled symbols represent the data recorded at 468 K in a temperature-ascending sequence (see text for details). The catalysts were purged with He while changing the reaction temperature.

In order to understand the deactivation, the activity with respect to onstream time (i.e., life test) at 468 K is examined and shown in Fig. 2 for three 10% Pd/C catalysts prepared from different precursor and support. The reaction temperature 468 K corresponds to the peak conversion temperature in Fig. 1. All three catalysts reveal similar onstream stability with a loss in benzene conversion of ca. 0.3 % h^{-1}. This indicates that the deactivation during the constant-temperature reaction test is not significant. This minor onstream activity loss shown in Fig. 2 cannot explain the deactivation observed in the temperature-ascending-descending sequence as shown in Fig. 1. Further-

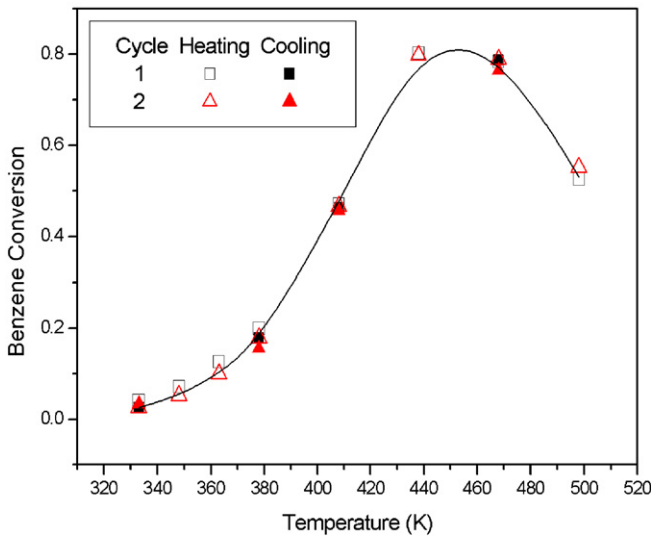

Fig. 4. Steady-state benzene conversion during a 2-cycle temperature-ascending-descending sequence of benzene hydrogenation over a 10% Pd/C catalyst. The Pd/C is prepared from $PdCl_2$ and XC72 support and is reduced by $NaBH_{4(aq)}$. In contrast to the conditions used in Fig. 1, the reaction gases were maintained at all time during temperature changes.

more, the measured conversions in life test were significantly lower than those measured at the same temperature during a temperature-ascending test sequence of the same catalysts; data from the temperature-ascending sequence are also shown in Fig. 2 for comparison. This indicates that the catalytic activity is determined mainly in the initial stage of reaction and is dependent on the reaction test procedure.

The effect of gas composition during reaction temperature changes is examined when applying the bracketing technique. One of the 10% Pd/C catalysts after a 24 h life test in Fig. 2 was tested again. Fig. 3 shows the reaction conversion using different gas atmosphere while varying temperature. Significant activity loss can be observed when hydrogen was excluded from purge gas during temperature variation. On the other hand, almost insignificant loss was found if the reaction gas is continuously flowing during temperature changes. This is confirmed in Fig. 4, in which 2 consecutive temperature-ascending-descending sequences as in Fig. 1 was performed but the reaction gas composition was maintained throughout the test. This indicates that Pd/C catalysts are stable under benzene hydrogenation gas environment. In contrast, the Pd/C showed deactivation when adopting the bracketing technique using He purge. From Figs. 3 and 4, the deactivation seems related to the sudden exposure to H_2-included gas stream and we use 'hydrogen-shock' hereafter to represent such a phenomenon.

The mentioned hydrogen-shock phenomenon suggests that catalyst deactivation can occur by H_2 pretreatment at elevated temperature, if the pretreatment is carried out by heating the catalyst under He, followed by H_2 introduction at the target temperature. We verify this in Fig. 5. The benzene hydrogenation activity is lower when a further H_2 treatment at 573 K is applied to the $NaBH_4$-reduced Pd/C catalysts from two Pd precursors. For Pd/C already reduced by $NaBH_{4(aq)}$, a further thermal treatment resulted in insignificant activity loss;

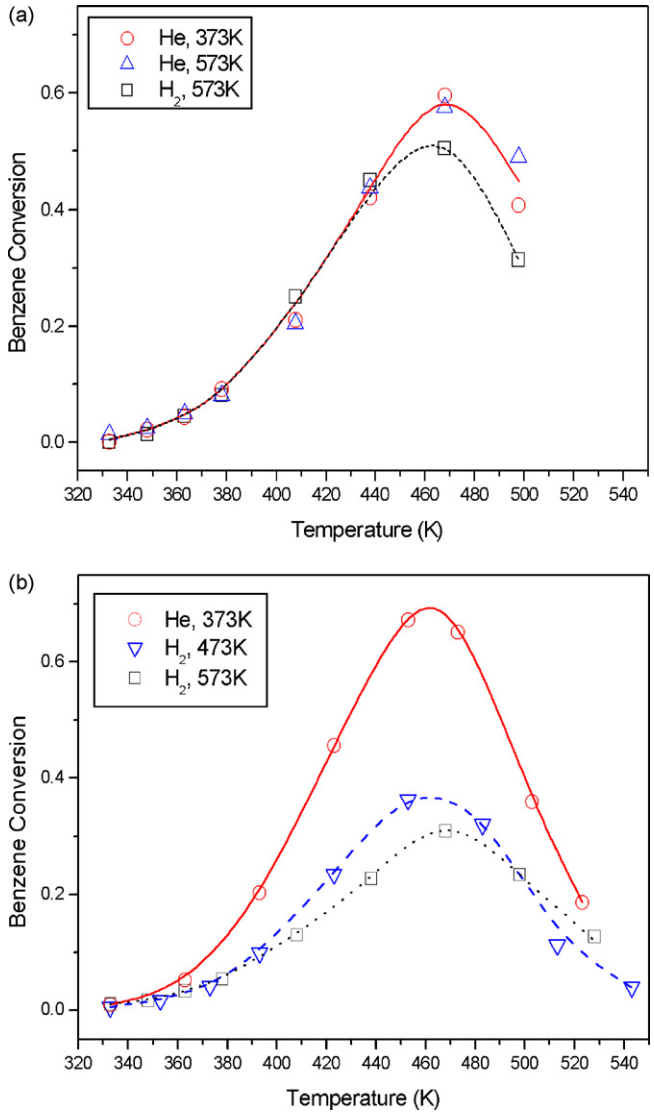

Fig. 5. Effect of gas pretreatment on benzene hydrogenation over $NaBH_4$-reduced 10% Pd/C prepared from (a) $PdCl_2$ precursor and XC72 support, and (b) $Pd(NO_3)_2$ precursor and XC72R support. Both catalysts were reduced by $NaBH_{4(aq)}$ prior to the on-line treatment.

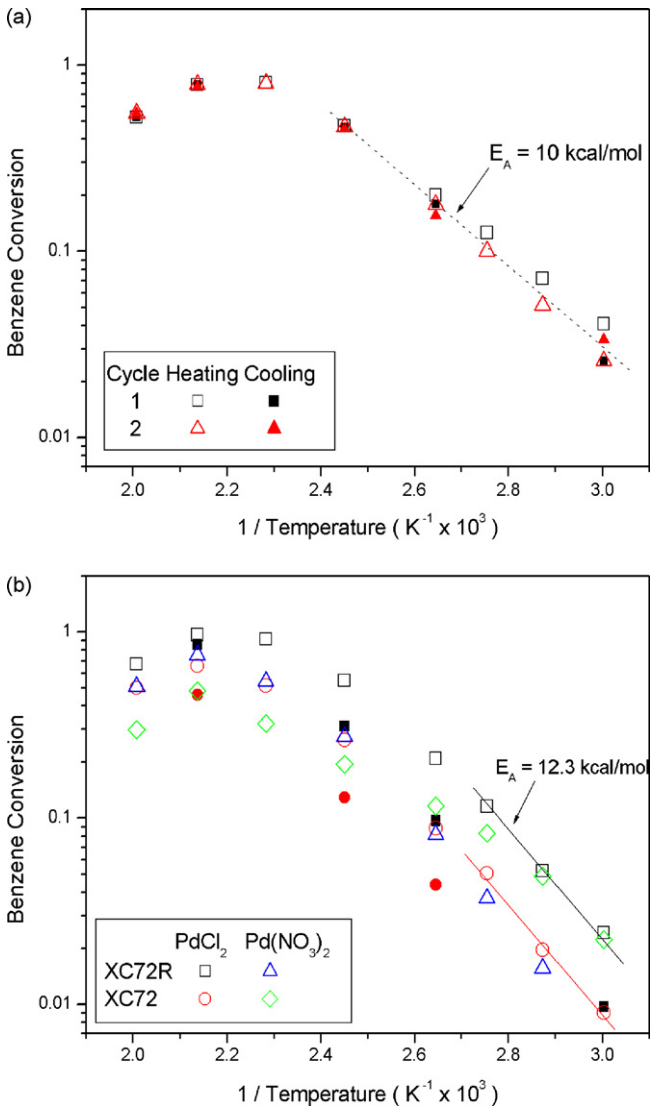

Fig. 6. Arrhenius plots of the benzene hydrogenation over 10% Pd/C catalysts: (a) from the 2-cycle temperature-ascending-descending sequence reported in Fig. 4, and (b) four $NaBH_4$-reduced Pd/C catalysts prepared from different Pd precursors and different carbon black supports.

whereas, a treatment by preheating the catalyst to a desired temperature and then introducing H_2 resulted in activity losses.

We can now delineate the kinetic performance of Pd/C. Fig. 6 shows the benzene conversion versus temperature in Arrhenius format. Fig. 6a shows the Arrhenius plot of the data in Fig. 4, i.e., the data without significant deactivation. An activation energy of ca. 10 kcal/mol describes the data. Fig. 6b is an Arrhenius plot of four $NaBH_4$-reduced 10% Pd/C catalysts from two precursors and two carbon supports, in which 'hydrogen-shock' is involved. The activation energy at the initial stage of the test sequence is similar for all four $NaBH_4$-reduced Pd/C catalysts, as ca. 12 kcal/mol. However, the activation energy may drops below 10 kcal/mol if high-temperature data are included in its calculation. This indicates that the apparent activation energy of the benzene hydrogenation over Pd/C is around 10–12 kcal/mol, similar to oxide-supported Pd and Pt catalysts [4,12]. When the deactivation occurs during the temperature-ascending sequence, activity data at higher temperatures would suffer more than those at lower temperatures, i.e., at the initial stage of the test sequence. Thus, the calculated activation energy from data covering a larger temperature range would be lower, as that reported for 1% Pd/C by Chou and Vannice [4].

Table 1 compares the benzene TOF at 363 K over all the Pd/C catalysts tested. The calculated TOFs are based on the CO chemisorption measurement before reaction tests and the reaction data at the initial stage of an identical temperature-ascending-descending procedure. All these Pd/C catalysts have similar TOFs, ca. 0.003–0.010 s^{-1} at 363 K. This is consistent with the TOFs of oxide-supported Pd catalysts at the same temperature [4,10]. The similar TOF and activation energy suggest that Pd/C and oxide-supported Pd catalysts have similar kinetic behavior during benzene hydrogenation.

3.2. Catalyst characterization

The EXAFS model fitting results of 10% Pd/C prepared from $PdCl_2$ and $Pd(NO_3)_2$ after different pretreatments are summarized in Table 2. Fresh catalysts contain mainly non-reduced Pd attributable to the precursor and a small fraction of metallic Pd phase. The presence of Pd–C interaction at a distance of ca. 3.6 Å has been discussed earlier [25,26]. Reduced and highly dispersed Pd is obtained after $NaBH_{4(aq)}$ reduction at 298 K. The presence of Pd–O coordination in the reduced Pd/C catalysts is attributed to the adsorbed oxygen because EXAFS measurements were done ex situ. This was verified by the absence of such Pd–O coordination in in situ EXAFS measurement of a H_2-reduced Pd/C [23]. The hydrogen reduction at 573 K resulted in larger Pd particles than the $NaBH_4$ reduction. A hydrogen treatment following the $NaBH_4$ reduction caused the Pd particle growth, as indicated by an increased Pd–Pd coordination number. A reduction in CO chemisorption is also observed in this case [23]. It has been discussed earlier in this paper that the H_2 treatment contributed to the deactivation by a 'hydrogen-shock' phenomenon. This suggests that 'hydrogen-shock' can cause Pd sintering. The Pd particle growth is also found after thermal treatment (He, 573 K for 1 h) following $NaBH_4$ reduction, but to a smaller extent than the hydrogen treatment. An increase in Pd–Pd coordination number is also found after benzene hydrogenation; the Pd–Pd coordination number increased more at higher reaction temperatures [25]. Comparatively, the highest Pd–Pd coordination number (i.e., the largest Pd particles) occurred when the fresh catalyst was directly reduced by H_2 at 573 K for all the catalysts analyzed in Table 2.

Particle growth is also observed in the 10% Pd/C after the 2-cycle benzene hydrogenation test reported in Fig. 1. Fig. 7 compares the TEM of 10% Pd/C before and after the 2-cycle reaction test. Both large (10–20 nm size) and small (ca. 2 nm) Pd can be found before the reaction test, in which the formation of large particles was most likely induced by the on-line H_2 treatment at 573 K before the reaction test. Comparatively, fewer small Pd particles are present after the reaction test. The smaller Pd particles on carbon surface seem to show a high tendency to sinter. The calculated particle size before and after the reaction test is 3.8 and 5.4 nm, respectively. This corresponds to a

Table 1
Benzene hydrogenation activities of differently prepared Pd/C catalysts

Catalyst					E_A (kcal/mol)	Activity at 363 K	
Precursor	Carbon	Pd (%)	Pretreatment	Pd_s/Pd		(μmol Bz/g/s)	TOF (s^{-1})
H_2PdCl_4	72	10	$NaBH_4$	0.12	13.0 ± 0.2	0.769	0.007
H_2PdCl_4	72	5	$NaBH_4$	0.29	12.7 ± 0.4	1.103	0.008
H_2PdCl_4	72	1	$NaBH_4$	0.29	9.6 ± 1.6	nil	nil
$Pd(NO_3)_2$	72	10	H_2, 573K	0.13	8.8 ± 1.3	0.622	0.005
$Pd(NO_3)_2$	72	10	$NaBH_4$	0.14	13.6 ± 0.1	0.942	0.007
$Pd(NO_3)_2$	72	10	$NaBH_4$(12)	0.24	12.2 ± 0.5	1.131	0.005
H_2PdCl_4	72R	10	$NaBH_4$	0.48	12.1 ± 0.8	2.067	0.005
H_2PdCl_4	72R	5	$NaBH_4$	0.45	11.2 ± 0.6	1.217	0.006
H_2PdCl_4	72R	1	$NaBH_4$	0.62	7.2 ± 0.4	0.182	0.003
H_2PdCl_4	72R	10	H_2, 573K	–	9.3 ± 0.9	0.989	–
H_2PdCl_4	72R	10	$NaBH_4$	0.27	10.3 ± 0.8	3.111	0.013
H_2PdCl_4	72R	10	$NaBH_4$(12)	–	12.8 ± 1.4	1.203	–
$Pd(NO_3)_2$	72R	10	$NaBH_4$	0.086	–	0.414	0.008

The Pd_s/Pd represent the Pd dispersion calculated based on CO chemisorption uptake at 298 K.

Table 2
EXAFS model regressions of differently prepared 10% Pd/C after different pretreatment

Sample	Shell	r (Å)	C.N.	σ^2	E_o (eV)	r-Factor
H_2PdCl_4/C(72R)						
Fresh	Pd–Cl	2.316 ± 0.004	3.7 ± 0.2	0.004 ± 0.0004	6.4 ± 1.0	0.016
	Pd–Pd	2.759 ± 0.023	0.5 ± 0.6	0.007 ± 0.006		
	Pd–C	3.553 ± 0.034	2.1 ± 2.2	0.003 ± 0.006		
$NaBH_4$	Pd–O	2.010 ± 0.005	1.5 ± 0.2	0.005 ± 0.0009	0.0 ± 0.4	0.002
	Pd–Pd	2.749 ± 0.002	5.2 ± 0.2	0.007 ± 0.0002		
	Pd–C	3.593 ± 0.020	1.9 ± 1.2	0.004 ± 0.004		
	Pd–Pd	3.873 ± 0.011	3.1 ± 1.1	0.013 ± 0.002		
$NaBH_4 + H_2$, 573 K	Pd–O	2.007 ± 0.017	0.7 ± 0.3	0.006 ± 0.004	−1.3 ± 0.5	0.003
	Pd–Pd	2.744 ± 0.002	7.5 ± 0.3	0.007 ± 0.0002		
	Pd–Pd	3.859 ± 0.011	5.7 ± 2.2	0.015 ± 0.003		
$NaBH_4 + N_2$, 573 K	Pd–O	2.001 ± 0.017	0.5 ± 0.3	0.002 ± 0.004	−1.9 ± 0.5	0.002
	Pd–Pd	2.740 ± 0.002	6.9 ± 0.5	0.007 ± 0.0004		
	Pd–Pd	3.857 ± 0.016	6.9 ± 3.5	0.017 ± 0.004		
H_2, 573K	Pd–O	2.019 ± 0.029	1.0 ± 0.8	0.011 ± 0.009	−1.6 ± 0.6	0.006
	Pd–Pd	2.740 ± 0.002	6.9 ± 0.4	0.007 ± 0.0003		
	Pd–Pd	3.854 ± 0.016	5.9 ± 3.1	0.016 ± 0.004		
H_2PdCl_4/C(72)						
Fresh	Pd–Cl	2.312 ± 0.006	3.3 ± 0.3	0.004 ± 0.0008	4.4 ± 1.1	0.007
	Pd–Pd	2.762 ± 0.008	1.0 ± 0.4	0.004 ± 0.002		
	Pd–C	3.608 ± 0.038	3.0 ± 2.9	0.006 ± 0.009		
$NaBH_4$	Pd–O	2.007 ± 0.009	1.1 ± 0.3	0.003 ± 0.002	−1.4 ± 0.7	0.001
	Pd–Pd	2.745 ± 0.003	5.6 ± 0.4	0.007 ± 0.0004		
	Pd–C	3.592 ± 0.027	2.0 ± 2.1	0.0001 ± 0.007		
	Pd–Pd	3.877 ± 0.021	5.3 ± 3.9	0.014 ± 0.007		
$Pd(NO_3)_2$/C(72R)						
Fresh	Pd–O	2.022 ± 0.015	3.1 ± 0.9	0.003 ± 0.003	4.8 ± 2.9	0.007
	Pd–Pd	2.749 ± 0.016	0.8 ± 0.8	0.003 ± 0.005		
	Pd–C	3.636 ± 0.032	4.2 ± 4.4	−0.0001 ± 0.007		
$NaBH_4$	Pd–O	1.985 ± 0.012	0.9 ± 0.3	0.006 ± 0.003	0.0 ± 0.4	0.004
	Pd–Pd	2.746 ± 0.002	5.9 ± 0.3	0.007 ± 0.0002		
	Pd–Pd	3.861 ± 0.015	4.4 ± 2.0	0.015 ± 0.004		
$NaBH_4 + H_2$, 573 K	Pd–O	2.009 ± 0.020	0.6 ± 0.4	0.005 ± 0.004	−1.0 ± 0.5	0.004
	Pd–Pd	2.744 ± 0.002	7.8 ± 0.4	0.007 ± 0.0002		
	Pd–Pd	3.862 ± 0.012	5.8 ± 2.5	0.014 ± 0.003		
H_2, 573 K	Pd–O	2.007 ± 0.021	0.7 ± 0.4	0.005 ± 0.004	−1.3 ± 0.5	0.004
	Pd–Pd	2.743 ± 0.002	7.9 ± 0.4	0.007 ± 0.0002		
	Pd–Pd	3.860 ± 0.014	6.7 ± 3.1	0.015 ± 0.004		

decreased dispersion from 0.3 to 0.21 by taking that dispersion = 1.13/d. For a structure-insensitive reaction, a loss of ca. 30% original activity would be expected. However, the activity loss in Fig. 1 is estimated as ca. 45 and 60%, respectively, at 378 and 463 K, from the data of the last temperature-descending sequence to that of the first temperature-ascending cycle.

Fig. 8 compares TGA data of the Pd/C catalyst before and after the 2-cycle reaction test in Fig. 1. Differential thermogravimetric spectra indicate that carbonaceous residue was presented and burned off at 463 and 673 K, respectively. The burn-off of carbon support occurred at 823 K. The weight loss feature at 1103 K corresponds to the conversion from PdO to Pd [27]. The carbonaceous residue may contribute to the catalyst deactivation in this study.

4. Discussion

In this study, Pd/C catalysts are found to subject to significant activity loss during benzene hydrogenation and deactivation is related to the operating procedure, e.g., that leads to the so-called H_2-shock phenomenon. The activity changes are insignificant for oxide-supported Pd catalysts when they are subjected to the same H_2-shock test procedure [23]. It indicates that the observed deactivation of Pd/C is related to the interaction between Pd and carbon support.

EXAFS results reported in Table 2 and that by Lin et al. [25] can provide information about the Pd/C deactivation phenomenon. The fresh impregnated Pd/C and the mildly reduced Pd/C catalysts by $NaBH_4$ show a Pd–C interaction at ca. 3.6 Å.

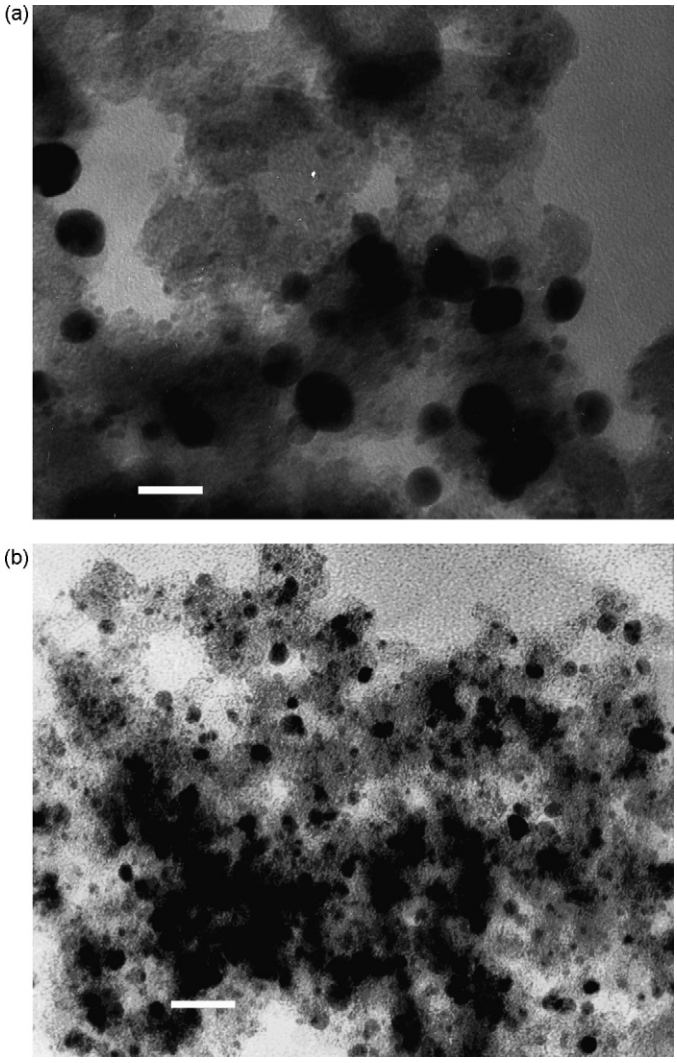

Fig. 7. TEM images of the 10% Pd/C catalyst (a) before and (b) after the 2-cycle benzene hydrogenation reaction test in Fig. 1. Scale bar in the photo represents 20 nm. The Pd/C catalyst is prepared from $PdCl_2$ precursor and XC72 carbon black, and is reduced by $NaBH_4$ followed by a H_2 treatment at 573 K.

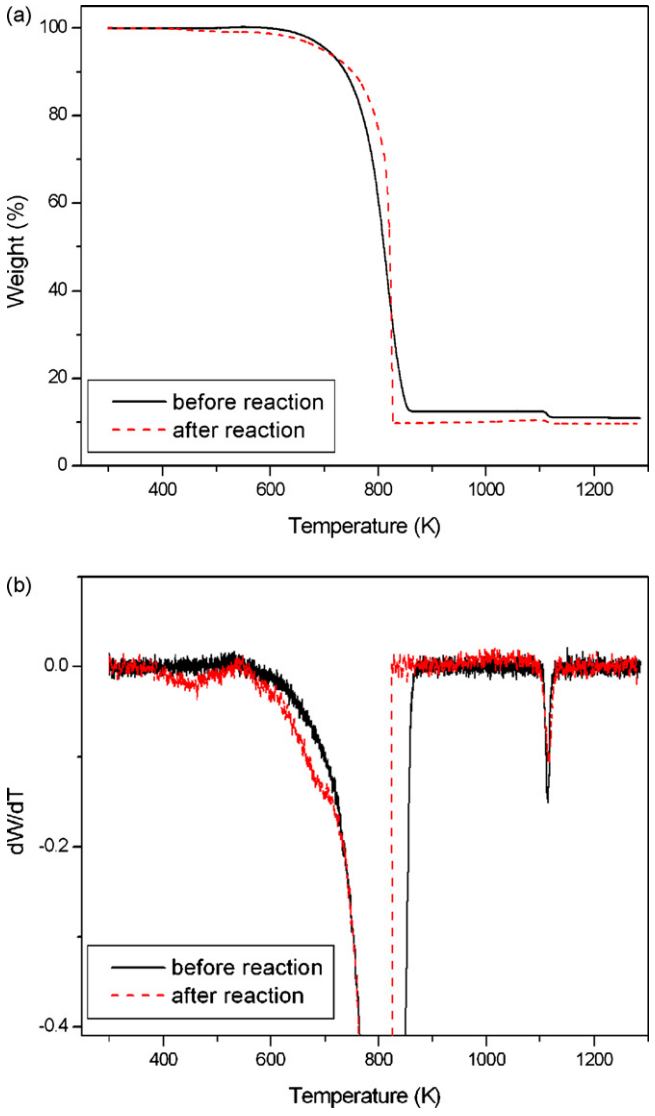

Fig. 8. (a) Thermogravimetry (TGA) and (b) differential thermogravimetry spectra of the 10% Pd/C catalyst before and after the 2-cycle benzene hydrogenation reaction test in Fig. 1. The Pd/C catalyst is prepared from $PdCl_2$ precursor and XC72 carbon black, and is reduced by $NaBH_4$ followed by a H_2 treatment at 573 K. The TGA analysis is performed under dry air at a heating rate of 2 K/min.

However, thermal heating, hydrogen treatment, and benzene reaction break down this Pd–C interaction causing the Pd–Pd coordination number to increase. This Pd–C interaction appears to be relatively weak and its disappearance can lead to Pd sintering.

Consequently, the loss of the Pd–C interaction is likely induced by the heat of hydrogen adsorption and absorption and the exothermic benzene reaction. The exothermic enthalpy from exposing Pd/C to reaction gas at 298 K includes: H_2 chemisorption (15–24 kcal/mol [16,28,29]), H_2 absorption (ca. 10 kcal/mol [16,28–31]), benzene adsorption (12–18 kcal/mol [5,32]) and reaction enthalpy (49 kcal/mol Bz). If the hydrogen is repeatedly stopped and flown during a benzene reaction test (i.e., using the bracketing procedure), the thermal fluctuation at the surface may be is significant. When the metal-support interaction is weak, Pd may lose its anchor and particle sintering can get worse through the temperature-ascending-descending test sequence. As described above, the consequence of the loss of Pd–C interaction include Pd sintering and catalyst deactivation. This qualitatively explains the different deactivation phenomena reported in Figs. 1 and 4. However, TEM analyses show that the change in Pd particle size cannot explain all of the activity loss in Fig. 1 and there must be another cause for the deactivation.

Krishnankutty and Vannice [17] proposed that carbon contamination to Pd nanocrystals is responsible for the suppression of H_2 chemisorption and benzene hydrogenation activity of Pd/C catalysts. Our EXAFS analyses show no Pd–C coordination at direct Pd–C bond distance at ca. 2 Å (as shown in Table 2 and in [25]). The Pd–O at ca. 2 Å in Table 2 is due to air exposure as described earlier and is not attributed to Pd–C. This indicates the absence of chemical interaction between Pd and C in Pd/C, even after a H_2-shock test procedure. If carbon

contamination is presented, only physical effect (e.g., surface site blocking) can be expected to cause the deactivation of Pd/C catalysts. This is consistent with Krishnankutty and Vannice [17], who reported that the carbon contamination would not change the heat of H_2 adsorption and absorption.

The carbonaceous residue observed in TGA (Fig. 8) may be viewed as the carbon contamination. The burn-off at 463 K probably corresponds to the oxidation temperature of benzene over Pd catalysts [33]. The burn-off feature at 673 K is attributed to more coke-like surface species. It is difficult to quantitatively estimate the amount of carbonaceous deposit directly from our TGA analysis. If the weight change from PdO to Pd at 830 °C in TGA is used and no loss of Pd is assumed, the back-calculated total carbonaceous residue is ca. 120 mg/g of the catalyst after the 2-cycle reaction in Fig. 1. This is equivalent to ca. 6 mg carbonaceous residue per m^2 of Pd surface based on a Pd dispersion of 0.3.

Another possibility is that a change in the morphology of Pd particles by the H_2-shock test procedure causes deactivation. Choukroun et al. [34] reported that the addition of H_2 can induce crystallization of PVP-protected Rh particles from polytetrahedral organization (amorphous) to fcc crystals. Polytetrahedral clusters can be expected to have a lower ratio of the second-shell to the first-shell metal–metal coordination when compared to the more crystalline phase. From Table 2, we can compare the ratio of second-shell to first-shell coordination before and after the H_2-shock caused by a further H_2-reduction at 573 K to the $NaBH_4$-reduced Pd/C. This ratio is increasing from 0.6 to 0.76 for the Pd/C prepared from H_2PdCl_4, but it remains nearly 0.74 before and after further H_2-reduction for catalysts prepared from $Pd(NO_3)_2$. It implies that a less crystalline phase was present in the $NaBH_4$-reduced Pd/C prepared from H_2PdCl_4, in which the Pd–C metal-support interaction is present. The H_2-shock procedure would cause the less crystalline phase to become more crystalline. However, such a crystallinity change is not considered as the main reason for the deactivation because the Pd/C from $Pd(NO_3)_2$ showed no crystallinity changes but the deactivation still occurs.

Pd/C catalysts have similar activation energy and similar TOFs as oxide-supported Pd catalysts when the deactivation is excluded from the analyses. We did such analyses by using only the data in the first few temperatures of the test sequence, which results are listed in Table 1. If the deviation from the expected kinetic performance (e.g., TOF and activation energy) can be used as an index to the extent of deactivation, Table 1 suggests that the lower metal loading catalysts suffer from a higher extent of deactivation. At the present time, it is not known if deactivation is caused by Pd sintering, carbonaceous residues, or a combination of both.

Pd precursor affects the characteristic of Pd/C catalysts, as the chemisorption suppression was observed in the Pd/C prepared from $Pd(acac)_2$ [17] but not from $PdCl_2$ precursors [18]. Figs. 5 and 6 demonstrates that the Pd/C prepared from $Pd(NO_3)_2$ precursor deactivates more severely than those prepared from H_2PdCl_4. Comparing the EXAFS fitting results in Table 2, the Pd–C interaction at 3.6 Å can be included in the fitting of the $NaBH_4$-reduced Pd/C from H_2PdCl_4 but not in that from $Pd(NO_3)_2$. This suggests that the Pd–C interaction in the fresh Pd/C prepared from $Pd(NO_3)_2$ is weaker than that prepared from H_2PdCl_4. A stronger Pd–C interaction would result in a more stable Pd/C catalyst. These results suggest that the overall kinetic performance of Pd/C catalysts and their morphology depends on the type of precursor. Though the detailed mechanism is not clear at this moment, the Pd–C interaction is important.

5. Conclusions

The benzene hydrogenation over Pd/C is found to show a stable onstream activity. However, the activity seems to be determined at the initial stage of the reaction test. When a bracketing technique is applied using a He purge during the temperature changes, severe deactivation is observed in a temperature-ascending-descending test sequence. On the other hand, no deactivation is found when the reaction gas (i.e., H_2 + benzene) is maintained throughout the test sequence. Similar phenomena are found in Pd/C prepared from different precursor and different carbon black supports. The activity and the stability of Pd/C during benzene hydrogenation are found to depend on the test procedure.

The deactivation is found to be accompanied by Pd sintering and the presence of carbonaceous residue. Sintering by itself is insufficient to account for the observed deactivation. The most likely reason for the Pd sintering is due to the loss of Pd–C interaction observed in EXAFS analysis. The effect of heat involved in repeatedly replacing hydrogen, as in the bracketing technique with a He purge, may deteriorate the Pd–C interaction. Pd/C prepared from different precursor have different tendencies toward deactivation, most likely due to the differences in Pd–C interaction strength. Consequently, the overall performance of Pd/C catalysts during hydrogenation can be affected by both the catalyst preparation and the operating conditions.

Acknowledgements

This study is partially supported by the National Science Council, Taiwan. Dr. J.-F. Lee of the National Synchrotron Radiation Research Center (NSRRC), Taiwan, ROC is acknowledged for his timeless help in EXAFS experiments. We thank one of the referees for mentioning the report of H_2-induced crystallization of Rh polytetrahedral particles and its reference.

References

[1] K.J. Yoon, P.L. Walker, L.N. Mulay, M.A. Vannice, Ind. Eng. Chem. Chem. Prod. Res. Dev. 22 (1983) 519.
[2] K.J. Yoon, M.A. Vannice, J. Catal. 82 (1983) 457.
[3] M.A. Vannice, W.C. Neikam, J. Catal. 23 (1971) 401.
[4] P. Chou, M.A. Vannice, J. Catal. 107 (1987) 129.
[5] P. Chou, M.A. Vannice, J. Catal. 107 (1987) 140.
[6] C. Leon, M.A. Vannice, Appl. Catal. 69 (1991) 305.
[7] M.V. Rahaman, M.A. Vannice, J. Catal. 127 (1991) 251.
[8] M.V. Rahaman, M.A. Vannice, J. Catal. 127 (1991) 267.

[9] N. Krishnankutty, M.A. Vannice, J. Catal. 155 (1995) 327.
[10] D. Poondi, M.A. Vannice, J. Catal. 161 (1996) 742.
[11] S.D. Lin, M.A. Vannice, J.M. Herrmann, D. Wang, C. Apestequia, D. Duprez, F. Figueras, W.C. Conner, S.L. Kiperman, W.K. Hall, D.G. Blackmond, W. Grunert, J.B. Butt, H. Schulz, Stud. Surf. Sci. Catal. 75 (Part A) (1993) 861.
[12] S.D. Lin, M.A. Vannice, J. Catal. 143 (1993) 539.
[13] S.D. Lin, M.A. Vannice, J. Catal. 143 (1993) 554.
[14] S.D. Lin, M.A. Vannice, J. Catal. 143 (1993) 563.
[15] U.K. Singh, M.A. Vannice, AIChE J. 45 (1999) 1059.
[16] P. Chou, Ph.D. Thesis, Penn State University, 1986.
[17] N. Krishnankutty, M.A. Vannice, J. Catal. 155 (1995) 312.
[18] N. Krishnankutty, J. Li, M.A. Vannice, Appl. Catal. A: Gen. 173 (1998) 137.
[19] R.F. Hicks, Q.-J. Yen, A.T. Bell, J. Catal. 89 (1984) 498.
[20] E.A. Stern, M. Newville, B. Ravel, Y. Yacoby, D. Haskel, Physica B 208–209 (1995) 117.
[21] S.I. Zabinsky, J.J. Rehr, A. Ankudinov, R.C. Albers, M.J. Eller, Phys. Rev. B 52 (1995) 2995.
[22] P. Weisz, Phys. Chem. NF 11 (1957) 1.
[23] P.-H. Jen, Master Thesis, Yuan Ze University, 2004.
[24] Y.-H. Hsu, Master Thesis, Yuan Ze University, 2004.
[25] S.D. Lin, Y.-H. Hsu, P.-H. Jen, J.-F. Lee, J. Mol. Catal. A 238 (2005) 88.
[26] B.L. Mojet, M.S. Hoogenraad, A.J. van Dillen, J.W. Geus, D.C. Koningsberger, J. Chem. Soc. Faraday Trans. 93 (1997) 4271.
[27] R.J. Farrauto, M.C. Hobson, T. Kennelly, E.M. Waterman, Appl. Catal. A 81 (1992) 227.
[28] P. Chou, M.A. Vannice, J. Catal. 104 (1987) 1.
[29] J.A. Konvalinka, J.J.F. Scholten, J. Catal. 48 (1977) 374.
[30] M. Watanabe, G. Wedler, P. Wissmann, Surf. Sci. 154 (1985) L207.
[31] C.H. Foo, C.T. Hong, C.T. Yeh, J. Chem. Soc. Faraday Trans. I 85 (1989) 65.
[32] C.G. Pope, J. Phys. Chem. 90 (1986) 835.
[33] J. Li, Z. Jiang, Z. Hao, X. Xu, Y. Zhuang, J. Mol. Catal. A 225 (2005) 173.
[34] R. Choukroun, D. de Caro, B. Chaudret, P. Lecante, E. Snoeck, New J. Chem. 25 (2001) 525.